# NEW OBSERVATIONS OF 3C382, 3C452 AND 3C465 AT 2.7 AND 5 GHz

J. M. Riley and N. J. B. A. Branson

(Received 1973 May 10)

# SUMMARY

The radio sources 3C 382, 3C 452 and 3C 465 have been mapped with the Cambridge One-Mile telescope at 2.7 and 5 GHz and with the Five-Kilometre telescope at 5 GHz. Each source has a central component less than 2" arc in diameter which is coincident with the nucleus of a galaxy, and outer components of considerable complexity. The extended components of 3C 452 and 3C 465 are significantly polarized. The observations are discussed in terms of different models for extended radio sources. None of the simple models can adequately account for all the observed features, but modifications of these models are proposed to obtain qualitative agreement with the observations. Several correlations between the physical properties of different extended sources are proposed.

#### I. INTRODUCTION

It has been known for some years that the greatest diversity in the structures of powerful extragalactic radio sources occurs amongst those at the lower end of the luminosity range ( $P_{178} \sim 10^{24}$ – $10^{26}$  W Hz<sup>-1</sup> sr<sup>-1</sup>), and for this reason each of these sources may provide separate clues to the physical processes occurring in such objects. With this in mind, observations have recently been made at high resolution with the Cambridge One-Mile and Five-Kilometre telescopes of the radio sources 3C 382, 3C 452 and 3C 465, which are known from previous observations ( $\mathbf{1}$ ,  $\mathbf{2}$ ,  $\mathbf{3}$ ) to have very complex extended radio structures; each one is associated with a galaxy of known redshift.

# 2. OBSERVATIONS

The present observations of 3C 382, 3C 452 and 3C 465 were made with the Cambridge One-Mile telescope (4) at 2.7 and 5 GHz. The main synthesized response of the telescope was a pencil beam with half-power beamwidths in right ascension of 12'' arc at 2.7 GHz and 6''.5 arc at 5 GHz; these beamwidths are increased in declination by a factor cosec  $\delta$ . Maps of the more compact regions of the sources were obtained at 5 GHz with the Five-Kilometre telescope (5), the half-power beamwidth being 2'' arc in right ascension and 2'' cosec  $\delta$  in declination.

For observations with the One-Mile telescope the interval a between individual aerial spacings was chosen so that the radius of the innermost grating ring  $(\lambda/a)$  exceeded the total angular extent of the source. The choice of a sets an upper limit of  $\sim \lambda/2a$  to the scale of angular structure which can be detected in the observations; structure in the source extending up to this limit is observed with little error (3). If N is the number of spacings used in the synthesis this limit is  $13'' \times N$  at 1.4 GHz,

 $7'' \times N$  at 2.7 GHz and  $4'' \times N$  at 5 GHz; the values of N are such that, except for the 1.4 GHz map of 3C 452, there should be little attenuation of large scale structure. This is borne out by the good agreement between the flux densities of each source obtained from the maps and those obtained using pencil beam instruments (6). For observations with the Five-Kilometre telescope no attempt was made to map the sources completely and only a few very compact regions were investigated; for each of these, mapping was complete over an area of sky of diameter 40'' arc.

It was sometimes useful to convolve the maps to larger beamwidths. This smoothing was effected by resynthesizing the maps omitting all the spacings larger than that required to give the desired resolution; the remaining spacings were weighted as usual (4) using a Gaussian distribution falling to 30 per cent at the maximum spacing.

All observations were made using linearly polarized feed horns: for the Five-Kilometre telescope the feeds were kept at position angle 90°, but for the One-Mile telescope the feeds were rotated every few minutes throughout the observations to position angles of 0°, 45° and 90° to enable linear polarization to be studied. The calibration and method of analysis of the polarization data is described by Mitton (24).

The scale of flux density was based upon values for the source 3C 147 given by Kellermann, Pauliny-Toth & Williams (6), namely  $13.0 \times 10^{-26}$  W m<sup>-2</sup> Hz<sup>-1</sup> at 2.7 GHz and  $8.2 \times 10^{-26}$  W m<sup>-2</sup> Hz<sup>-1</sup> at 5 GHz.

In the discussion of each source, physical parameters have been derived for the various components. It is assumed that all redshifts are cosmological in origin, and that an Einstein–de Sitter cosmology may be employed. The value of Hubble's constant is assumed to be 50 km s<sup>-1</sup> Mpc<sup>-1</sup>. Estimates are given of the minimum energy in the radio components; it is assumed that all radio emission is caused by synchrotron radiation from relativistic electrons, and that there is equipartition between the energies of the relativistic particles and of the magnetic field. It is assumed that radio emission extends over the frequency range 10–10 000 MHz, and that energy in the form of relativistic protons is unimportant. The following formula has been used:

Minimum energy = 
$$2.0 \times 10^{55} P^{4/7} V^{3/7} 500^{4\alpha/7} \left[ \frac{0.316 - 10^{(1-3\alpha)}}{2(2\alpha - 1)} \right]^{4/7} \text{ erg}$$

where P is the radio luminosity at 5 GHz in units of  $10^{23}$  W Hz<sup>-1</sup> sr<sup>-1</sup>, and V is the volume of the component in units of  $10^{66}$  cm<sup>3</sup>. Values of the corresponding equipartition magnetic fields are also given.

# 3. RESULTS AND COMMENTS

3.1 3C 382

(a) Results. The 5 GHz map of 3C 382 shown in Fig. 1 was made with the One-Mile telescope at 32 interferometer spacings. The central component of the source (B) is unresolved and is less than o"·5 arc, that is o·8 kpc, in diameter; it is coincident with the  $14^{m}$ ·5 D3 galaxy (z = 0.0586 (7)) identified (8) with the source, and is presumably associated with the nucleus of the galaxy. The preceding component (A) has no compact structure and is peculiar in having a low brightness 'tail' about 1 minute of arc in extent at  $45^{\circ}$  to the line joining the component to

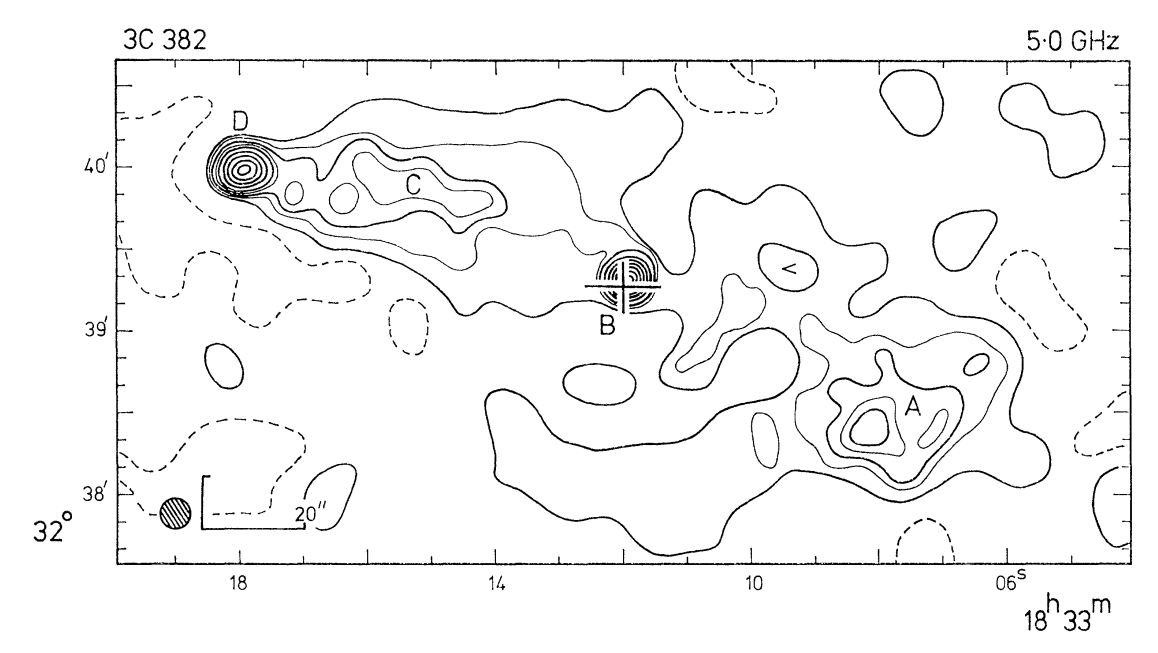


Fig. 1. Map of 3C 382 at 5 GHz. The declination scale is compressed by a factor  $\sin \delta$ , so that the telescope beam appears circular. The arms of the L shape are of equal angular size indicating the extent of the compression. 1950.0 coordinates are used. The contour interval is 48 K; the thin lines represent contours at half this interval. The half-power beamwidth is shown in the bottom left-hand corner of the map. The cross marks the position of the D3 galaxy identified with the source; the size of the cross shows the approximate extent of the galaxy.

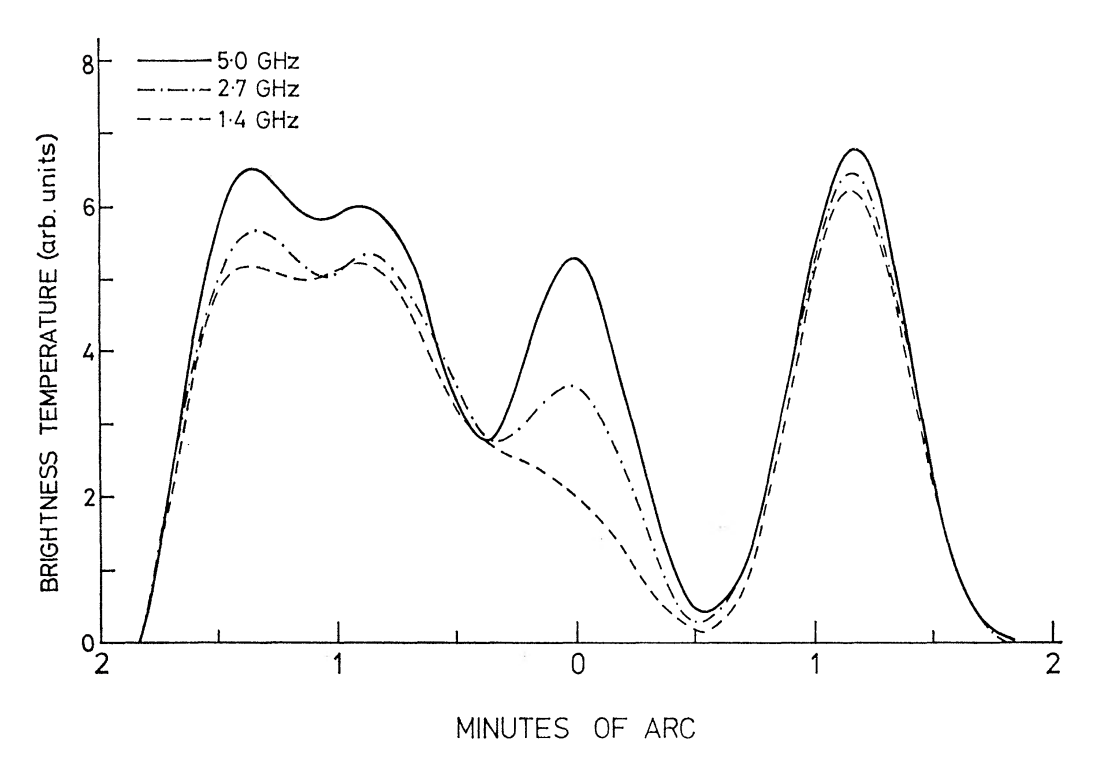


Fig. 2. Profiles of brightness temperature along the major axis of 3C 382 at 1.4, 2.7 and 5 GHz, each smoothed to the same beamwidth, corresponding to a resolution of 23" arc in right ascension. The units of brightness temperature are arbitrary at each frequency.

the galaxy; this feature has also been observed on the maps made at 1.4 and 2.7 GHz. The following component has a compact region (D) and a broad extensive low brightness region (C) between this and the galaxy. Component D has been mapped with the Five-Kilometre telescope; it has angular half-widths of 3" north—south and 3".5 east—west, with the leading edge unresolved.

A comparison of the present observations at 5 and 2.7 GHz with those previously obtained at 1.4 GHz (3), at eight interferometer spacings, shows that the overall structure of the source is very similar at the three frequencies. Profiles of brightness temperature along the major axis of the source are shown in Fig. 2; each profile has a resolution in right ascension of 23" arc. Each of the two outer components has a spectral index  $\alpha$  (defined as  $S \propto \nu^{-\alpha}$ ) of 0.74, whereas the central component associated with the galaxy has a spectral index of 0.0±0.2.

Details of the various components are listed in Table I: the quantities  $\omega_{\parallel}$  and  $\omega_{\perp}$  refer to the half-power widths of the components parallel and perpendicular to their major axes.

No significant polarization has been found, allowing upper limits of  $\sim 15$  per cent at 2.7 GHz and  $\sim 30$  per cent at 5 GHz to be placed on the polarization of components A and D.

Table I
3C 382 components

	Position	(1950.0)		
	R.A.	Dec.	$\omega_{\parallel}$ $\omega_{\perp}$	$T_{ m b}({ m K})$
Component	h m s $\pm$ s	° ' " ±"	(" arc) (" ar	c) 5.0 GHz
A	~ 18 33 o8	~32 38 30	20 20	87
$\mathbf{B}$	18 33 11.63 0.01	32 39 18.9 0.1	<o.5 <o<="" td=""><td>·5 &gt; 46 ooo</td></o.5>	·5 > 46 ooo
C	~ 18 33 15	~32 39 50	30 20	83
D	~ 18 33 17.92	~32 39 58.2	3.2	950

3C 382 flux densities

		Flux d	lensities (:	10 <sup>-26</sup> W	m <sup>-2</sup> Hz <sup>-1</sup> )	ı	_	ctral lex
Component	$S_{1\cdot 4}$	土	$S_{2\cdot 7}$	土	$S_{5\cdot 0}$	土	α	土
A	1.6	0.5	1.1	0.3	0.7	0.1	0.74	0.03
В	0.3	0.1	0.22	0.03	0.53	0.03	0.0	0.2
C	)		)		1.0	0.5	)	
	3.7	0.2	2.2	0.4			0.74	0.03
D	J		)		0.20	0.03	J	

3C 382 physical parameters of components

Component	z	Distance (Mpc)	$P_{5.0} \ ( ext{10}^{23}   ext{W Hz}^{-1}   ext{sr}^{-1})$	Minimum energy (10 <sup>56</sup> erg)	Magnetic field (10 <sup>–5</sup> Gauss)
A	0.0586	336	8 · 4	71	1.1
${f B}$			2.8	0.1	11.0
C			12.0	104	1.1
$\mathbf{D}$			2.4	3.5	3.6

- (b) Comments. The important features of these observations are as follows:
- (i) There is a very compact central component coincident with the nucleus of the galaxy indicative of continuing activity in the galaxy. This effect, in which

the compact central component of a radio source has a significantly flatter spectrum than the outer components, has been noted for several other radio sources, for example the N-galaxies 3C 390.3 (9), and 3C 109 (10) and the quasi-stellar source 3C 47 (10).

(ii) The easterly component (D) has a compact leading edge with a low brightness 'tail' (C) extending back towards the galaxy. This structure appears similar to that predicted by ram pressure models of source confinement. However, calculations such as those of Christiansen (II) show that the maximum width of the tail should be less than  $2\pi$  times the scale height of the exponential atmosphere in the component, which would be approximately the same as the radius of the high brightness region which is only  $\sim 3''$  arc. Accordingly the breadth of the tail ( $\sim 50''$  arc) is greater than would be predicted by strict application of the ram pressure models. A similar problem also arises in modified ram pressure models which include backward diffusion of the relativistic electrons (I2) and instabilities in the individual components (I3).

In models of radio sources in which low frequency waves are continuously supplied from the nucleus (14), the existence of a component 'tail' might be attributed to radio emission from a tube or waveguide down which energy is being carried to the source component; again this theory is not consistent with the present observations as the tube cannot be wider than the component it is supplying.

A more realistic model for the structure of radio source components involving the continuous supply of relativistic matter from the nucleus has been developed by Scheuer (1973, in preparation). In this model, account is taken of the fact that components consisting entirely of relativistic particles must expand at a velocity limited by the ram pressure of the ambient intergalactic gas; the accelerated particles inflate a cavity of relativistic matter enclosing both the tube, down which the energy is supplied, and the galaxy; Scheuer suggests that these particles may give rise to the extended regions of emission behind components. If ram pressure is the only containment mechanism, the cavity is cigar-shaped, but if the thermal pressure of the intergalactic gas dominates along the sides of the cavity, it is possible that the cavity could take up the sort of configuration observed in the tail of 3C 382. It is significant that the energy density in the tail is  $\sim 10^{-11}$  erg cm<sup>-3</sup>, so that confinement is possible by an intergalactic gas of density  $2 \times 10^{-4}$  cm<sup>-3</sup> and temperature  $\sim 10^8$  K, such as might be found in a cluster of galaxies (15). It should however, be noticed in this context, that it appears likely that 3C 382 is at most in a very small group of galaxies.

It is possible that the structure of the western component (A), which has no compact regions, has developed as a result of the dissolution, perhaps by the growth of instabilities (13), of a component similar to the eastern one. The energy density in this component is such that containment could also be produced by the thermal pressure of the intergalactic gas. The remarkable bent tail of this component could then be attributed to large scale motions in such a gas.

(iii) It is interesting that the two main components of the source are so different. Possible reasons for this asymmetry include large differences in the density of the intergalactic gas on opposite sides of the galaxy, an asymmetry in the original explosion, and a continuing supply of energy from the central component to the eastern component, but not to the western one. There seems to be no way of distinguishing these at present.

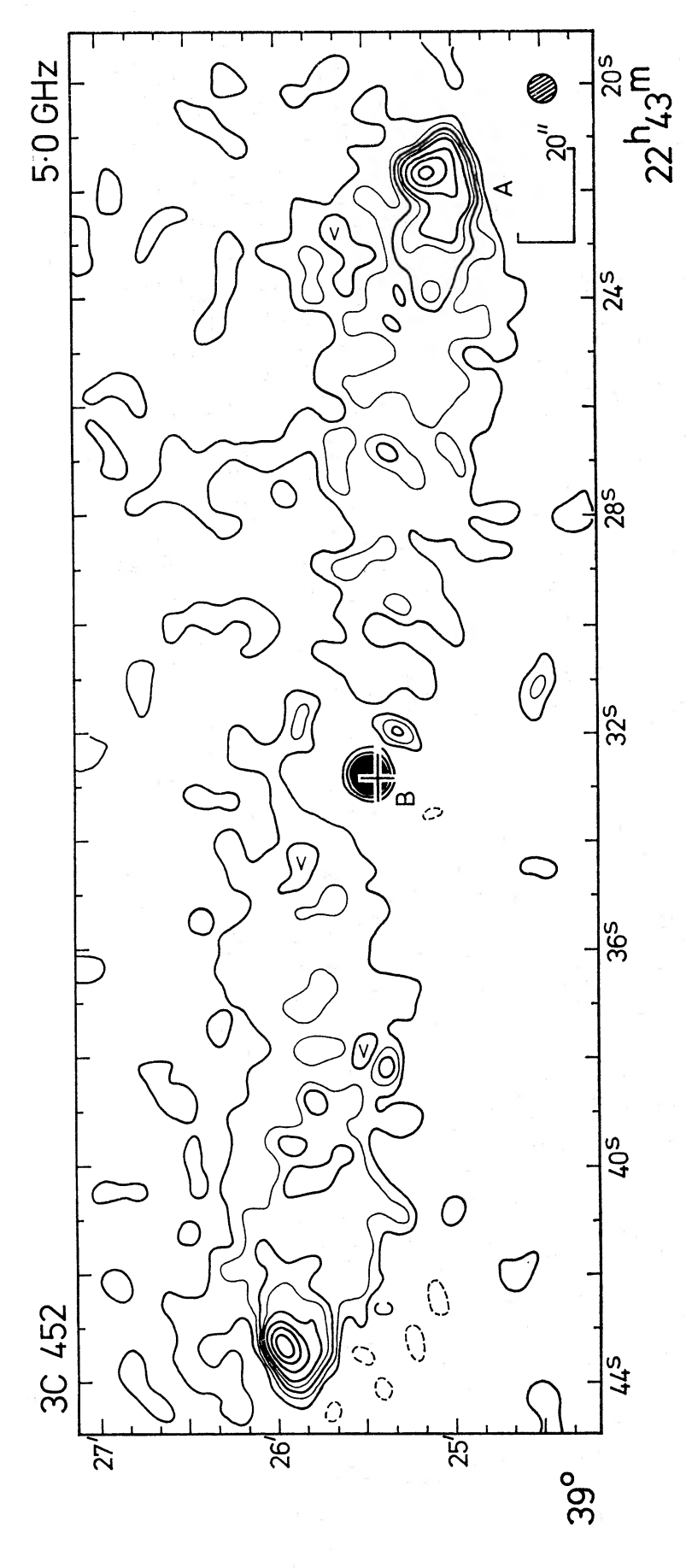


FIG. 3. Map of 3C 452 at 5 GHz. The contour interval is 27 K; the thin lines represent contours at half this interval. The half-power beamwidth is shown in the bottom right-hand corner of the map. The cross marks the position of the ED galaxy identified with the source; the size of the cross shows the approximate extent of the galaxy.

3.2 3C 452

(a) Results. The radio source has been identified (8) with a 16<sup>m</sup> ED galaxy having a redshift of 0.0820 (7), which is probably the member of a cluster (16). The present observations at 5 GHz are shown in Fig. 3; the map is that obtained with the One-Mile telescope with 64 interferometer spacings. The central component (B) is unresolved and is less than 0".5 arc, that is 1.0 kpc, in diameter; it is probably coincident with the galactic nucleus, although the positions given by Véron (17) and Griffin (18) differ by more than the beamwidth of the Five-Kilometre telescope (2" arc).

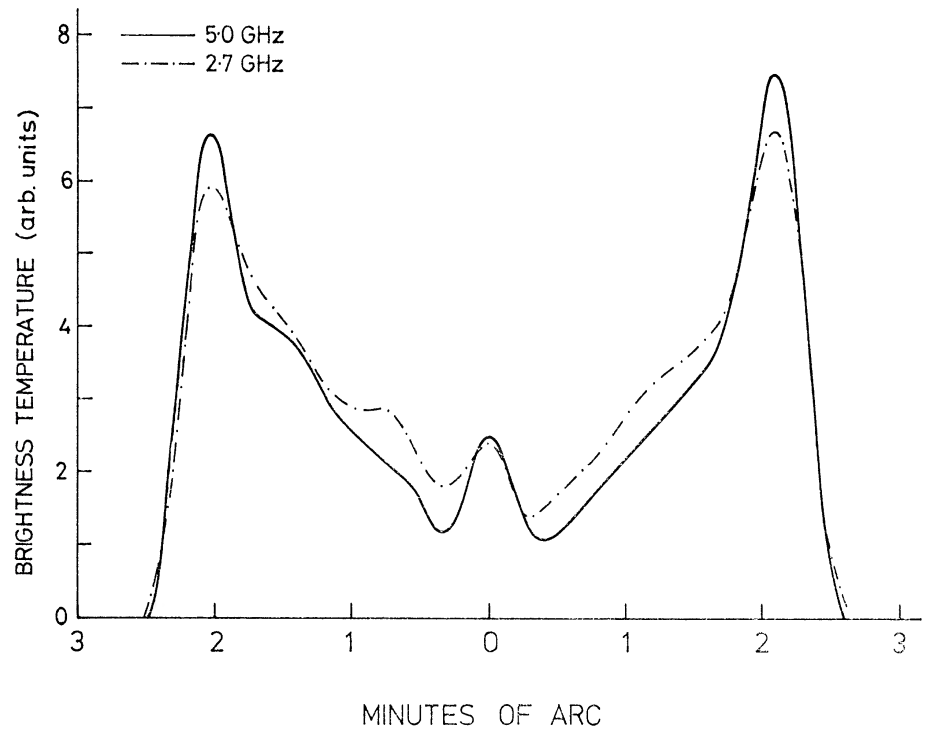


FIG. 4. Profiles of brightness temperature along the main axis of 3C 452 at 2.7 and 5 GHz, both smoothed to the same beamwidth corresponding to a resolution of 23" arc in right ascension.

A comparison of the present observations at 5 and 2.7 GHz with those previously obtained at 1.4 GHz ( $\mathbf{r}$ ), at eight interferometer spacings, shows that the overall structure of the source is similar at the three frequencies. Profiles of brightness temperature at 2.7 and 5 GHz along the major axis of the source are shown in Fig. 4; each profile has a resolution in right ascension of 23'' arc. The outer components of the source have lower spectral indices ( $\sim 0.5$ ) than the inner tail regions ( $\sim 0.85$ ), but the central component associated with the galaxy has a still lower spectral index of  $0.1 \pm 0.3$ , a value similar to that found for the central component of 3C 382.

Details of the various components are listed in Table II.

The present observations have revealed significant polarization in the radio emission at 2.7 GHz; the distributions of linearly polarized flux density and polarization angle at 2.7 GHz are shown as a vector map in Fig. 5 convolved to a beamwidth of 47" arc in right ascension. It is clear from this figure that most of the polarized emission comes from the inward extensions of the source and not from

# TABLE II

# 3C 452 components

	ŀ	osition	(1950.	0)				
	R.A.			Dec.		ω∥	$\omega_{\perp}$	$T_{ m b}({ m K})$
Component	h m s	$\pm s$	0	, "	± "	(" arc)	(" arc)	5.0 GHz
$\mathbf{A}$	~22 43 22		~ 39	25 10		~ 30	20	150
В	22 43 32.81	0.01	39	25 27.66	0.10	<0.2	<0.2	> 26 000
C	~22 43 43		~ 39	25 50		~ 30	20	125

# 3C 452 flux densities

		index						
Component	$S_{1\cdot 4}$	土	$S_{2\cdot 7}$	土	$S_{5\cdot 0}$	土	α	±
$\mathbf{A}$	6.3	0.7	3.1	0.4	ı · 8	0.3	0.9	0.1
В	<0.3		0.14	0.03	0.13	0.03	0.1	0.3
C	5.3	0.7	2.7	0.4	1.2	0.3	0.9	0.1

# 3C 452 physical parameters of components

Component	z	Distance (Mpc)	$P_{5 \cdot 0}$ (10 <sup>23</sup> W Hz <sup>-1</sup> sr <sup>-1</sup> )	Minimum energy (10 <sup>56</sup> erg)	Magnetic field (10 <sup>–5</sup> Gauss)
$\mathbf{A}$	0.0820	462	43	450	1.4
В			2.8	0.3	9.1
C			36	410	1.3

the two more compact components. The vectors are aligned over more than one beam area indicating that the magnetic field is ordered over  $\sim 100$  kpc. The observations are not sensitive enough to show details of the polarization at 5 GHz though it is possible to obtain information on the integrated polarization of the

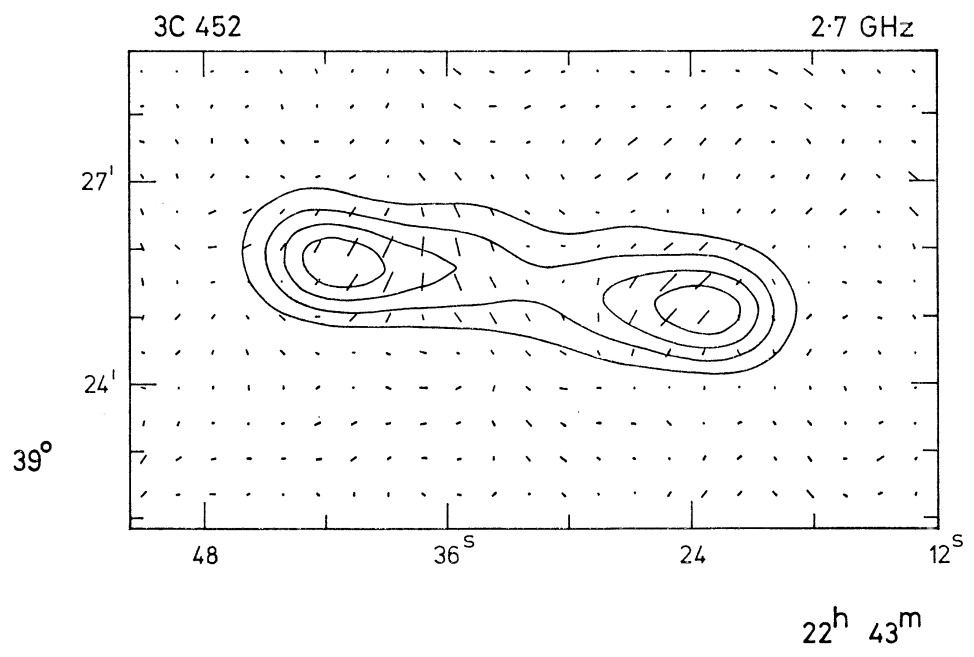


Fig. 5. Map of 3C 452 at 2.7 GHz with a resolution of 47" arc in right ascension, together with vectors showing the polarized flux density; the longest vector on the map represents a polarized flux density of  $0.15 \times 10^{-26}$  W  $m^{-2}$  Hz<sup>-1</sup> per beam area (1.0 square minutes of arc). The position angle is that of the electric vector.

two components. Previous measurements of the net polarization of the source at these frequencies (19, 20) are consistent with the present distributions.

The distribution of polarization at 1.4 GHz has previously been determined with a similar resolution to that in Fig. 5 by Baldwin et al. (21). Values of the percentage polarization and the position angle at 1.4 GHz and 2.7 GHz are given in Table III for points along the main axis of the source every two seconds in right ascension. These results indicate that there is considerable depolarization throughout the west component and little in the east component in the frequency range 2.7-1.4 GHz.

The 5-GHz results for the integrated polarization of each component indicate that there is not much depolarization between 5 and 2.7 GHz in either component. The intrinsic polarization of the extended regions of each component is thus ~15 per cent which suggests (22) that ~30 per cent of the total magnetic field is uniform.

Table III

Polarization along the main axis of 3C 452

0 2 2 2 7 7 7 7			J J - TJ -	
2·7 GHz	1.4 GHz	2.7 GHz	1·4 GH	$\mathbf{z}$
%	%	p.a.	p.a.	
0 ± 2	0 ± 2	-		
4±2	$3 \pm 1$	30	135	
5 ± 2	$3 \pm 1$	140	135	_
$13 \pm 2$	$5\pm 1$	135	135	strong depolarization
$15 \pm 3$	0 ± 2	140		strong depolarization
9 ± 3	5 ± 2	160	45	
< 4	$6\pm 2$		45	
$5\pm3$	14±2	20	45	~
17±2		20	50	
	$18 \pm 1$	5	45	little depolarization
$16\pm3$	$12 \pm 1$	170	30	fittle depolarization
$12\pm2$	$9 \pm 1$	150	6	J
$8\pm 2$		150	-	
9 ± 2	$5\pm 2$	140	22	
	$0 \pm 2$ $4 \pm 2$ $5 \pm 2$ $13 \pm 2$ $15 \pm 3$ $9 \pm 3$ $< 4$ $5 \pm 3$ $17 \pm 2$ $18 \pm 3$ $16 \pm 3$ $12 \pm 2$ $8 \pm 2$	2.7 GHz 1.4 GHz  % % 0 $\pm$ 2 0 $\pm$ 2 4 $\pm$ 2 3 $\pm$ 1 5 $\pm$ 2 3 $\pm$ 1 13 $\pm$ 2 5 $\pm$ 1 15 $\pm$ 3 0 $\pm$ 2 9 $\pm$ 3 5 $\pm$ 2 <4 6 $\pm$ 2 5 $\pm$ 3 14 $\pm$ 2 17 $\pm$ 2 16 $\pm$ 1 18 $\pm$ 3 18 $\pm$ 1 16 $\pm$ 3 12 $\pm$ 1 12 $\pm$ 2 9 $\pm$ 1 8 $\pm$ 2 —	2.7 GHz       1.4 GHz       2.7 GHz         %       %       p.a.         0 $\pm 2$ 0 $\pm 2$ —         4 $\pm 2$ 3 $\pm 1$ 30         5 $\pm 2$ 3 $\pm 1$ 140         13 $\pm 2$ 5 $\pm 1$ 135         15 $\pm 3$ 0 $\pm 2$ 140         9 $\pm 3$ 5 $\pm 2$ 160         <4	2.7 GHz       1.4 GHz       2.7 GHz       1.4 GHz         %       %       p.a.       p.a.         0 $\pm$ 2       —       —       —         4 $\pm$ 2       3 $\pm$ 1       30       135         5 $\pm$ 2       3 $\pm$ 1       140       135         13 $\pm$ 2       5 $\pm$ 1       135       135         15 $\pm$ 3       0 $\pm$ 2       140       —         9 $\pm$ 3       5 $\pm$ 2       160       45         <4

- (b) Comments. The important features of these results are as follows:
- (i) There is a compact central component with properties similar to those of the central component of 3C 382.
- (ii) The source was originally considered to be an example of a quadruple source with two pairs of components—the result of two well-defined events in the galaxy. It is now clear that the inner components are merely extensive low brightness tails attached to the outer ones, contributing ~80 per cent of the flux at 5 GHz. In producing a model for this source with its extensive low brightness regions, the same considerations apply as for the eastern component of 3C 382; in 3C 452, however, the ratios of the widths of the tails to the dimensions of the high brightness regions are probably smaller, so the basic ram pressure model fits better. Again, the energy densities in the tail regions are ~ 10<sup>-11</sup> erg cm<sup>-3</sup>, so that confinement could be effected by the external pressure of the intergalactic gas, and a model similar to that suggested for the eastern component of 3C 382 may be able to produce such tails.

(iii) The more compact outer regions of each component have lower spectral indices than the inner regions. This phenomenon has been observed in several other extended double sources, notably Cygnus A (23), 3C 61.1 (10) and 3C 274.1 (3). The mechanism usually proposed to explain such spectral variations is that in the regions of low spectral index the spectrum represents the injection spectrum of the particles, whilst in the regions of high spectral index it represents the spectrum of the particles after modification by significant energy losses.

The problem with this interpretation in the case of 3C 452 is that the overall spectrum of the source is straight over the range 38 MHz-5 GHz (6) with a spectral index of 0.85, and the inner components dominate even at 5 GHz; thus it appears that the inner components have a fairly constant spectral index of 0.85 over the above frequency range. Any model thus has to be carefully specified: not only must the electrons, now radiating at frequencies ≤ 100 MHz in the tails. have lost significant energy during the source lifetime to steepen the low frequency spectrum, but also some 5-GHz electrons must still remain in the tails to prevent the high frequency spectrum from steepening catastrophically. A simple model to account for this is one in which the particles are continuously accelerated in the compact outermost regions and then diffuse into the tails. The lifetimes of all particles radiating at frequencies above ~ 100 MHz are assumed to be less than the lifetime of the source. The situation is then the classic one of continuous injection with continuous energy loss by synchrotron (or inverse compton) radiation; the spectral index of the tail would then be 0.5 greater than that of the compact outermost region. The lifetime of the source must thus be at least 108 yr (assuming a magnetic field of 10<sup>-5</sup> Gauss in the tails) which implies a velocity of translation of the components of less than o.o. c.

(iv) There is a striking difference in the rates of depolarization taking place in the two components, in spite of their symmetry on the total intensity map. It is possible that the depolarization in the west component is due to differential rotation across the component over scales smaller than the beam area used here (1 square minute of arc), as proposed by Mitton for Cygnus A (24). It is also possible, however, that the depolarization is due to differential Faraday rotation along a line of sight through the source (22); if Burn's model for depolarization (22) is assumed, the internal rotation measures of the west and east components must be  $\sim$  40 and  $\leq$  10 rad m<sup>-2</sup> respectively. Furthermore, if the path length through the source is 40 kpc and a uniform longitudinal magnetic field of  $3 \times 10^{-6}$  Gauss is present, the above values suggest particle densities of  $\sim 3 \times 10^{-4}$  and  $\sim 8 \times 10^{-5}$  cm<sup>-3</sup> in the west and east components, respectively. An alternative, and perhaps more likely, explanation of the difference in the rotation measures is that it is due to a difference in the angles which the smooth magnetic field makes to the line of sight for each component. The mass of thermal matter in each component must be  $\sim$  10<sup>8</sup>-10<sup>9</sup>  $M_{\odot}$ .

The depolarization implies that, whatever its origin, there are significant variations in rotation measure across the source. In view of this, there is no reason to expect the variation of the position angle of the integrated polarization of 3C 452 with wavelength  $\lambda$ , to fit a  $\lambda^2$  law, and consequently it seems unlikely that the anomalously high overall rotation measure of  $-272 \pm 10$  rad m<sup>-2</sup> quoted for the source (25) has any physical significance.

Unfortunately the large errors in the individual position angle measurements for the components make it possible to fit several apparently possible rotation measures to each component, all of which are consistent with the results for the

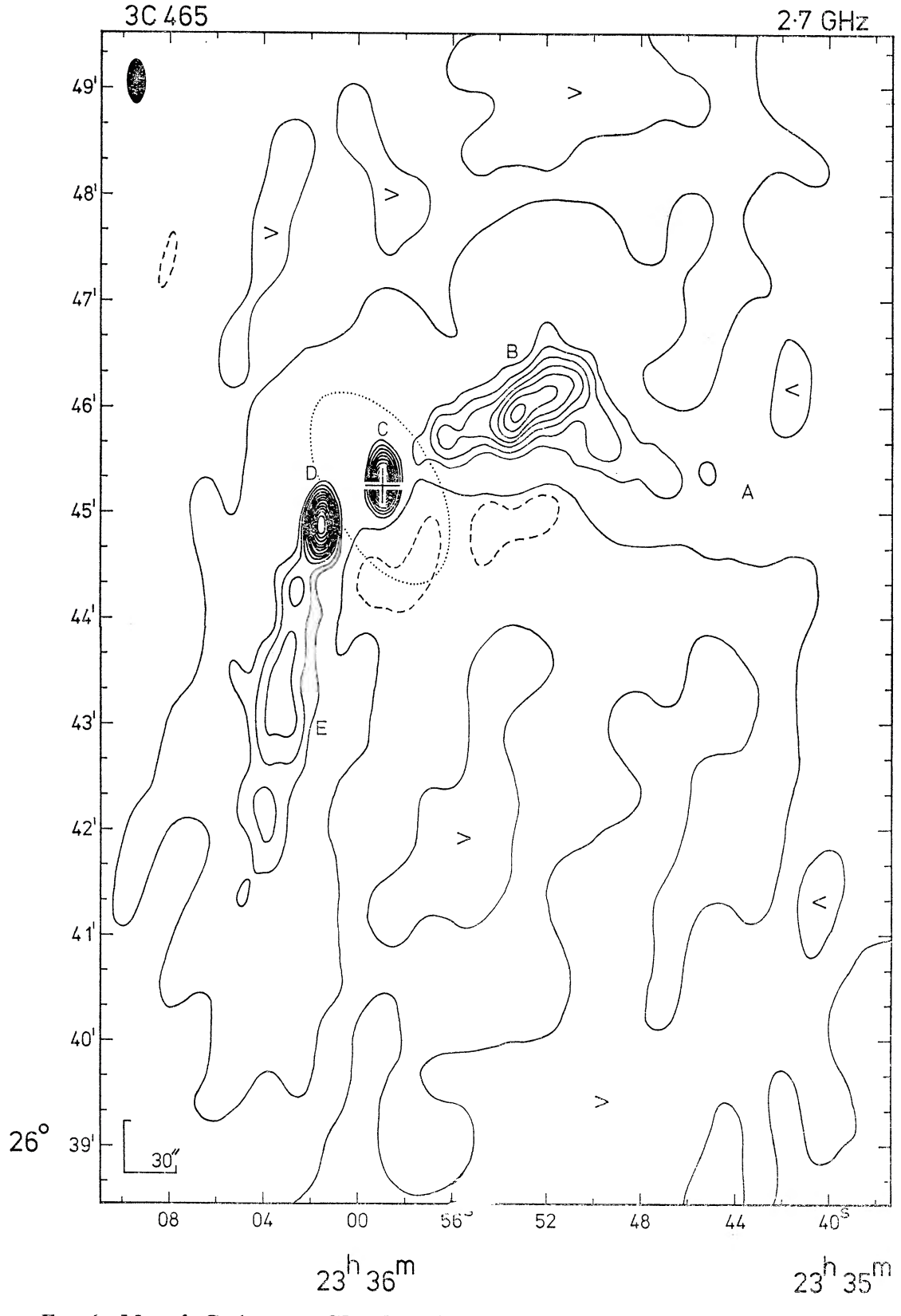


Fig. 6. Map of 3C 465 at 2.7 GHz shown in sky coordinates. The contour interval is 17 K. The half-power beamwidth is shown in the top left-hand corner of the map. The cross marks the position of the southern component of NGC 7720; the dotted line shows the approximate extent of the galaxy.

integrated polarization. At the position of the source  $(l = 98^{\circ}, b = -17^{\circ})$  the Galaxy could be responsible for a rotation of up to  $\sim -80$  rad m<sup>-2</sup> (26) and with the uncertainty in the Galactic contribution it is not possible to derive the intrinsic position angles of polarization in the individual components unambiguously.

# 3.3 3C 465

(a) Results. The radio source 3C 465 is associated with the 12<sup>m</sup>·2 cD4 galaxy NGC 7720 (7) in the cluster Abell 2634. Previous radio observations (2) at 408 and 1407 MHz, with 16 interferometer spacings, have shown that it is a complex source of very large angular size (~10' arc) with several distinct components. It is quite unlike most double radio sources both because the brighter compact radio components are closer to the galaxy than the extended components, and because the components do not lie even approximately on a straight line.

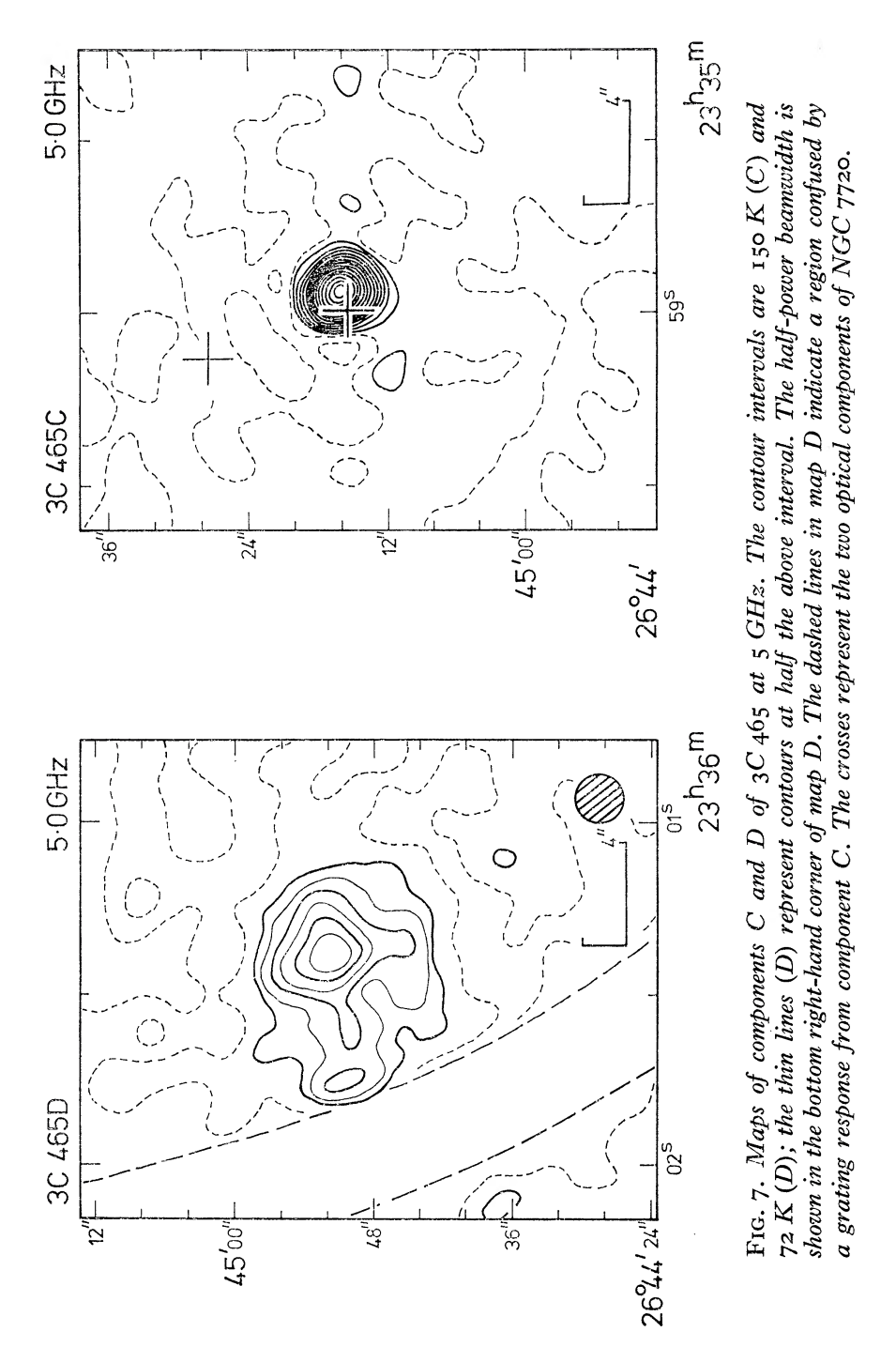
The present observations were made with the One-Mile telescope at 64 interferometer spacings which is adequate to map the complete source at 2·7 GHz and all the structure up to 4'·5 arc in size at 5 GHz; the Five-Kilometre telescope was used to map components C and D at the centre of the source. The 2·7 GHz map is shown in Fig. 6 and the 5 GHz maps of components C and D in Fig. 7. The details of the various components are given in Table IV.

An upper limit of about 2" arc can be placed on the angular size of component C; this component is coincident with the brighter southern component of NGC 7720 (18). This galaxy consists of two optical components in a common envelope; the southern component has a weak emission line spectrum as well as an absorption spectrum, while the northern component has only an absorption spectrum (8). The highly elliptical envelope is of enormous extent, the major axis being more than 2' arc in extent on the Sky Survey print, which at the redshift of the galaxy (0.0301) corresponds to  $\sim 100$  kpc. The major axis is in position angle  $\sim 30^{\circ}$  and the envelope is asymmetrical being extended towards the south-west. There are several other galaxies in the cluster whose projected images lie close to the radio source, and five whose images actually lie within it; these show no sign of optical peculiarity so it is difficult to say how, if at all, they are related to the source.

Components B and D lie on a line approximately perpendicular to the major axis of the galaxy and any bridge of radio emission connecting them to component C is extremely faint. It is likely that component D and the central regions of B lie within the galaxy; in this respect they resemble the inner regions of 3C 66 (27). Components E and B are both very extended being fairly narrow near the galaxy and widening out like the north-following component of 3C 66. Component B ends fairly abruptly 2' arc from the galaxy when it spreads out slightly to the north and continues strongly to the south-west.

The considerable spectral index variations over the source can be seen clearly in Fig. 8. Component C has a spectral index of 0.0, B and D about 0.6, A about 1.3 and E about 1.0; the general trend is for the spectral index to increase with distance from the galaxy.

The distributions of linearly polarized flux density and polarization angle at 2.7 GHz are shown as a vector map in Fig. 9 convolved to a beamwidth of 23" arc in right ascension. There is strong polarization in the extended components of the source, reaching 40 per cent in some regions. The percentage polarization and position angle of the electric vectors are shown in Table V for each component of



284.

# TABLE IV

# 3C 465 components

	Pos	sition (195	0.0)				
	R.A.		Dec.		$\omega_{\parallel}$	$oldsymbol{\omega}_{\perp}$	$T_{\mathrm{b}}(\mathrm{K})$
Component	h m s	± s	) <i> </i>	± "	(" arc)	(" arc)	5.0 GHz
$\mathbf{A}$	~23 35 44	~ 2	6 45 30		50	20	5
В	~23 35 52	~ 2	6 46 00		40	20	23
C	23 35 58.95	0.01 5	6 45 16.44	0.10	~2	<0.2	> 14 500
D	23 36 01.48	2	6 44 51.6		8	ΙΙ	170
E	~23 36 03	~ 2	6 43 20		250	25	6

# 3C 465 flux densities

		-	Spectral index					
Component	$S_{1\cdot 4}$	土	$S_{2\cdot 7}$	$\pm$	$S_{5\cdot 0}$	<u>±</u>	α	土
$\mathbf{A}$	0.30	0.12	0.10	0.03	0.13	0.02	1.3	0.6
$\mathbf{B}$	2.93	0.30	1.75	0.30	1.30	0.13	0.63	0.02
C	0.30	0.03	0.58	0.03	0.29	0.03	0.00	0.03
D	0.65	0.02	0.43	0.04	0.30	0.03	0.60	0.02
E	3.03	0.30	1.31	0.11	0.87	0.10	1.06	0.06

# 3C 465 physical parameters of components

Component	<i>&amp;</i>	Distance (Mpc)	$P_{5\cdot0}$ (10 <sup>23</sup> W Hz $^{-1}$ sr $^{-1}$ )	Minimum energy (10 <sup>56</sup> erg)	Magnetic field (10 <sup>–5</sup> Gauss)
A	0.0301	176	0.4	33	1.1
В	_		4.0	39	0.7
$\mathbf{C}$			0.8	0.02	9.2
D			o·8	2.0	i · 6
$\mathbf{E}$			2.8	130	o·8

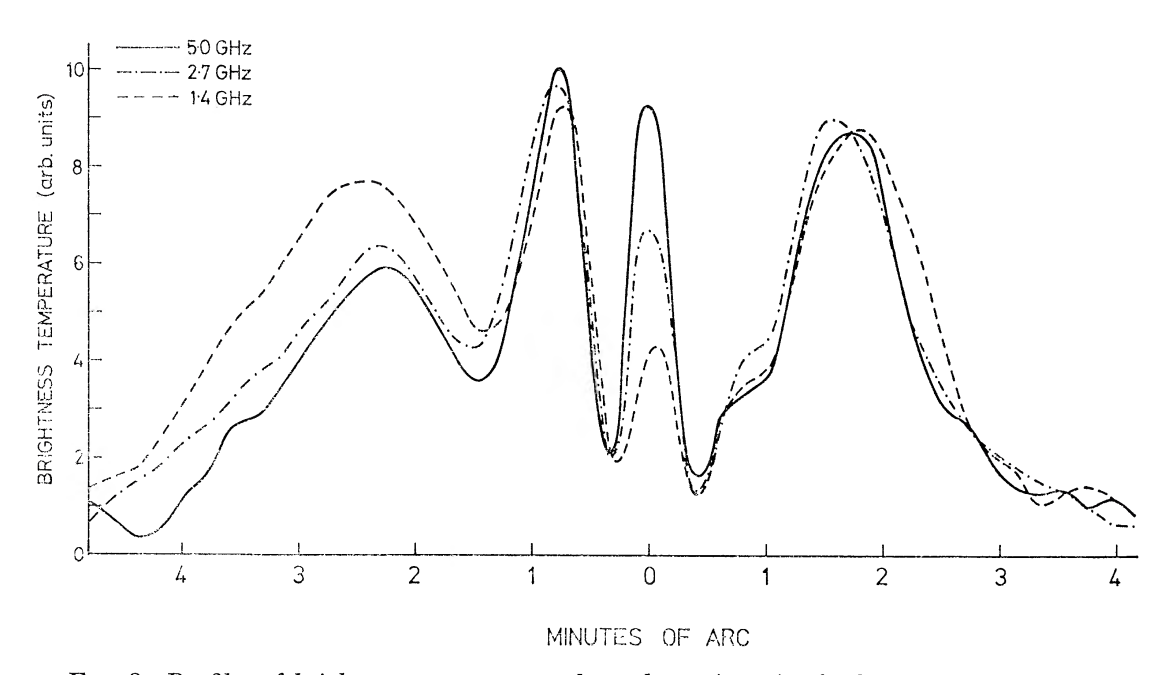


Fig. 8. Profiles of brightness temperature along the main axis of 3C 465 at 1.4, 2.7 and 5 GHz, each smoothed to the same beamwidth, corresponding to a resolution of 23" arc in right ascension.

the source at 2.7 and 5 GHz. The more compact components C and D show little polarization whereas the extended components B and E are very highly polarized. In these components there is roughly a  $-30^{\circ} \pm 10^{\circ}$  rotation between 5 and 2.7 GHz corresponding to a rotation measure of  $-60 \pm 20$  rad m<sup>-2</sup>. Studies of the Galactic

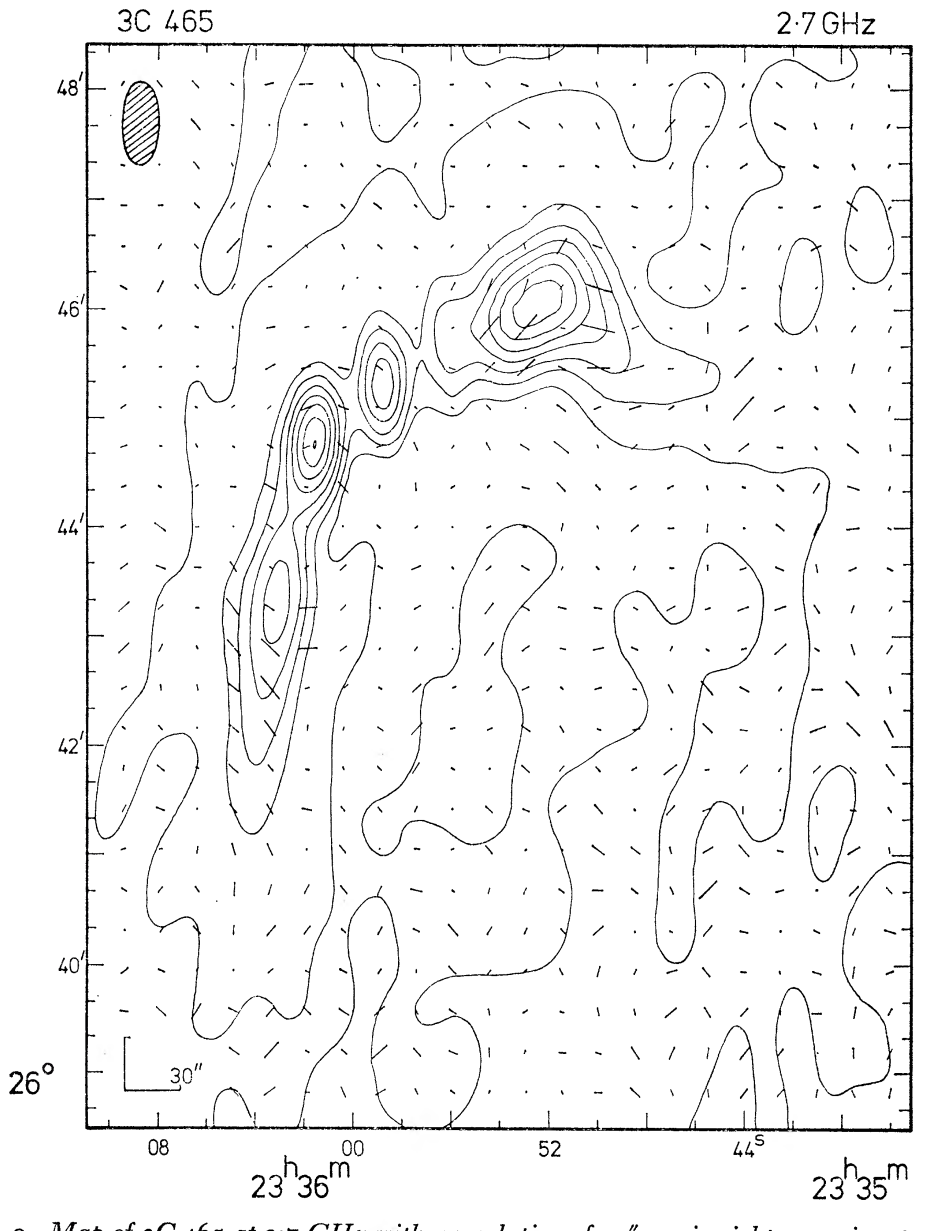


FIG. 9. Map of 3C 465 at 2.7 GHz with a resolution of 23" arc in right ascension, together with vectors showing the polarized flux density; the longest vector on the map represents a polarized flux density of  $0.09 \times 10^{-26}$  W  $m^{-2}$  Hz<sup>-1</sup> per beam area (0.26 square minutes of arc).

distribution of rotation measures (26) indicate that at the position of 3C465 ( $l=103^{\circ}$ ,  $b=-35^{\circ}$ ) the Galaxy could contribute a large fraction, if not all, of this rotation. The intrinsic position angle of the electric vectors is everywhere approximately perpendicular to the axis of the source; if it is assumed that the radiation is by the synchrotron mechanism, the associated magnetic field must be parallel to the source axis. The percentage polarizations at 5 and 2.7 GHz are the

same, to within experimental error, and indicate that the strength of the uniform and random components of the magnetic field in the very extended regions of the source are comparable.

Table V

Polarization in 3C 465

							Intrinsic p.a.	
Component	2.7 (	$_{ m GHz}$	5.0 (	GHz	2.7 GHz	5.0 GHz	$\mathbf{of}$	P.a. of source
h m s	%	土	%	$\pm$	p.a.	p.a.	polarization	axis
$\int 23 \ 35 \ 49$	29	6	40	12	86	133	153	50
$B \begin{cases} 23 & 35 & 49 \\ 23 & 35 & 54 \end{cases}$	16	4	20	8	150	177	188	120
C	7	4	6	6			*******	
D	8	6	18	10		50		
E	19	4	31	10	45	70	80	170

- (b) Comments. The interesting features of these observations are as follows:
- (i) The central component has a completely flat spectrum between 1·4 and  $5~\mathrm{GHz}$ .
- (ii) There is no compact structure far from the centre of the galaxy; in this respect this source resembles other weak extended sources, notably 3C 66 (27), 3C 129 and 3C 83.1B (28). The energy densities outside the associated galaxy in all such sources are such that confinement can be effected by the external pressure of an intergalactic gas of density  $\sim 2 \times 10^{-4}$  cm<sup>-3</sup> and temperature  $\sim 10^{8}$  K. It could then be supposed that the bent structure of 3C 465 is produced as a result of large scale motions within this intergalactic gas.
- (iii) There are considerable spectral index variations over the source with the spectrum steepening with increasing distance from the galaxy; this tendency is observed in the other weak extended sources mentioned above. In this respect these sources differ from the more 'typical' double sources (such as 3C 452) in which, in general, if variations occur, the spectral index increases towards the centre of the galaxy; in each case, however, the regions of higher spectral index are the regions of lower energy density.
- (iv) The polarization measurements indicate that there is a highly ordered magnetic field running approximately along the axis of the source. The percentage polarization increases with increasing distance from the galaxy, as observed in the 'head-tail' sources 3C 129 and IC 310 (29).

# 4. SUMMARY OF CONCLUSIONS

It is thought that the most significant features of the sources discussed in this paper are as follows:

- (a) Each source has a very compact central component, with a flat spectrum between 1.4 and 5 GHz, coincident with the nucleus of the associated galaxy.
- (b) Both 3C 382 and 3C 452 exhibit very extended bridges of low brightness emission between the outermost components and the centre; the energy densities in these bridges are such that confinement could be effected by the thermal pressure of the intergalactic gas.
- (c) In both 3C 382 and 3C 452 the outermost components have been resolved with the exception of one edge of each of the north-following components.

- (d) 3C 465 shows little fine structure except very close to the centre of the galaxy.
- (e) 3C 452 and 3C 465 show considerable variations of spectral index; in 3C 452 the spectral index increases towards the centre of the galaxy whereas in 3C 465 the value increases markedly with increasing distance from the centre. In both cases, however, the regions of low energy density are the regions of high spectral index.
- (f) Both 3C 452 and 3C 465 show very considerable polarization in the extended regions, indicating highly ordered magnetic fields in the regions of low energy density.

# ACKNOWLEDGMENTS

We thank the members of the Radio Astronomy group who assisted in making the observations, and Dr M. S. Longair for helpful discussion during the preparation of this paper.

Mullard Radio Astronomy Observatory, Cavendish Laboratory, Cambridge

# REFERENCES

- (I) Ryle, M., Elsmore, B. & Neville, A. C., 1965. Nature, 207, 1024.
- (2) Macdonald, G. H., Neville, A. C. & Ryle, M., 1966. Nature, 211, 1241.
- (3) Macdonald, G. H., Kenderdine, S. & Neville, A. C., 1968. Mon. Not. R. astr. Soc., 138, 259.
- (4) Elsmore, B., Kenderdine, S. & Ryle, M., 1966. Mon. Not. R. astr. Soc., 134, 87.
- (5) Ryle, M., 1972. Nature, 239, 435.
- (6) Kellermann, K. I., Pauliny-Toth, I. I. K. & Williams, P. J. S., 1969. Astrophys. J., 157, 1.
- (7) Schmidt, M., 1965. Astrophys. J., 141, 1.
- (8) Matthews, T. A., Morgan, W. W. & Schmidt, M., 1964. Astrophys. J., 140, 35.
- (9) Harris, A. B., 1972. Mon. Not. R. astr. Soc., 158, 1.
- (10) Branson, N. J. B. A., Elsmore, B., Pooley, G. G. & Ryle, M., 1972. Mon. Not. R. astr. Soc., 156, 377.
- (II) Christiansen, W., 1969. Mon. Not. R. astr. Soc., 145, 327.
- (12) Mills, D. M. & Sturrock, P. A., 1970. Astrophys. Lett., 5, 105.
- (13) Blake, G. M., 1972. Mon. Not. R. astr. Soc., 156, 67.
- (14) Rees, M. J., 1971. Nature, 229, 312.
- (15) Gursky, H., Kellogg, E., Murray, S., Leong, C., Tananbaum, H. & Giacconi, R., 1971. Astrophys. J., 167, L81.
- (16) Wyndham, J. D., 1966. Astrophys. J., 144, 459.
- (17) Véron, P., 1966. Astrophys. J., 144, 861.
- (18) Griffin, R. F., 1963. Astr. J., 68, 421.
- (19) Seielstad, G. A., 1967. Astrophys. J., 147, 24.
- (20) Sastry, Ch. V., Pauliny-Toth, I. I. K. & Kellermann, K. I., 1967. Astr. J., 72, 230.
- (21) Baldwin, J. E., Jennings, J. E., Shakeshaft, J. R., Warner, P. J., Wilson, D. M. A. & Wright, M. C. H., 1970. *Mon. Not. R. astr. Soc.*, 150, 253.
- (22) Burn, B. J., 1966. Mon. Not. R. astr. Soc., 133, 67.
- (23) Mitton, S. A. & Ryle, M., 1969. Mon. Not. R. astr. Soc., 146, 221.
- (24) Mitton, S. A., 1971. Mon. Not. R. astr. Soc., 153, 133.
- (25) Berge, G. L. & Seielstad, G. A., 1967. Astrophys. J., 148, 367.
- (26) Mitton, S. A., 1972. Mon. Not. R. astr. Soc., 155, 373.
- (27) Northover, K. J. E., 1973. Mon. Not. R. astr. Soc., in press.
- (28) Riley, J. M., 1973. Mon. Not. R. astr. Soc., 161, 167.
- (29) Miley, G. K., 1973. Astr. Astrophys., in press.